



**UNIVERSITI PUTRA MALAYSIA**

**POTENTIOSTATIC AND PULSE ELECTRODEPOSITON OF  
COPPER SELENIDE THIN FILMS**

**KOO CHEE SIONG  
FS 2009 38**



**POTENTIOSTATIC AND PULSE ELECTRODEPOSITON OF  
COPPER SELENIDE THIN FILMS**

**By**

**KOO CHEE SIONG**

**Thesis submitted to the School of Graduate Studies, Universiti Putra Malaysia,  
in Fulfilment of the Requirements for the Degree of Master**

**2009**



Dedicated to my beloved parents and Shiau Hun



Abstract of thesis presented to the Senate of Universiti Putra Malaysia in fulfilment of the requirement for the degree of Master of Science

**POTENTIOSTATIC AND PULSE ELECTRODEPOSITON OF  
COPPER SELENIDE THIN FILMS**

By

**KOO CHEE SIONG**

**October 2009**

**Chairman: Professor Zulkarnain Zainal, PhD**

**Faculty: Science**

Copper selenide attracts much interest due to its potential applications in photovoltaic devices, rechargeable lithium battery, superionic conductor, ion selective microelectrode and as a precursor to prepare  $\text{CuInSe}_2$ . Among the synthesis methods for copper selenide, electrodeposition is relatively simple, cost-effective, and low temperature growth technique. However, previously no detailed studies on electrodeposition parameters of this metal chalcogenide have been carried out. On the other hand, pulse electrodeposition of copper selenide has never been reported. In present work, copper selenide thin films were electrodeposited onto indium tin oxide coated glass (ITO) in acidic aqueous solution containing  $\text{CuSO}_4$  and  $\text{Na}_2\text{SeO}_3$  via potentiostatic and a novel pulse technique from a three-electrode cell.

The electrode processes and potential range of copper selenide deposition were studied by cyclic voltammetry. Characterisation of the films was performed using X-ray Diffractometry (XRD), Photoelectrochemical Test (PEC) and Scanning Electron Microscopy (SEM). Optical band gap and transition type of the copper selenide were

determined using UV-vis Spectrophotometer. Electrochemical properties of CuSe and Cu<sub>3</sub>Se<sub>2</sub> rich phase deposits were also investigated by solid state voltammetry technique. The samples were also annealed under nitrogen atmosphere at different temperatures and characterised.

Potentiostatic deposition was carried out at different deposition potentials, Na<sub>2</sub>SeO<sub>3</sub> concentrations, deposition time, pH and bath temperatures. XRD patterns manifested the increases of deposition potential from -0.1 V to -0.6 V, Na<sub>2</sub>SeO<sub>3</sub> concentrations from 0.006 M to 0.01 M, deposition duration from 1 min to 25 min and bath temperature from 0 °C to 55 °C favors the growth of CuSe phase relative to Cu<sub>3</sub>Se<sub>2</sub>. However, longer deposition time, high potential and bath temperature resulted to poor adherent films. Copper selenide was deposited at pH 1.25-2.25 to avoid the formation of Cu<sub>2</sub>O. Most preparative parameters did not significantly influence the photoactivity of the as-grown deposits. The pH and annealing temperature strongly affected the photosensitivity of the samples.

Pulse electrodeposition was performed by varying cathodic pulse potentials and duty cycle. Pulse technique can access the potential up to -0.9 V to deposit good adherent films. Increasing pulse potential and duty cycle promoted the growth of CuSe phase rather than Cu<sub>3</sub>Se<sub>2</sub>. However, most deposits were not sensitive to light.

The films preparative parameters of both approaches were optimized based on their photosensitivity. All samples are polycrystalline in nature and exhibited p-type semiconducting character in photoelectrochemical test. Annealing at 400 °C causes the formation of Cu<sub>2-x</sub>Se. The sequential pulse-deposited and annealed deposit

contained  $\text{Cu}_2\text{O}$  impurity which decreased the direct gap of  $\text{Cu}_{2-x}\text{Se}$  from 1.98 eV to 1.36 eV and improved the photocurrent significantly.

The SEM micrographs of potentiostatic and pulse plated as-grown deposits at selected potential show well covered, crack and pinhole free surface morphology. The roughness and particle sizes of copper selenide increase with increasing potentials in each case. Pulse-deposited films have comparatively smoother surface morphology and smaller particles size. The electrochemical properties of deposit with CuSe as the majority phase clearly differ from  $\text{Cu}_3\text{Se}_2$  rich deposit in solid phase voltammetry study.

Abstrak tesis yang dikemukakan kepada Senat Universiti Putra Malaysia  
sebagai memenuhi keperluan untuk ijazah Master Sains

**ELEKTROENAPAN POTENTIOSTATIK DAN DENYUTAN LAPISAN  
FILEM NIPIS KUPRUM SELENIDA**

Oleh

**KOO CHEE SIONG**

**Oktober 2009**

**Pengerusi: Profesor Zulkarnain Zainal, PhD**

**Fakulti: Sains**

Kuprum selenida menarik minat disebabkan potensi kegunaannya dalam peranti fotovoltan, bateri litium yang dapat dicas semula, konduktor superionik, mikroelektrod pilihan ion dan sebagai bahan mentah untuk penyediaan  $\text{CuInSe}_2$ . Antara kaedah-kaedah sintesis bagi kuprum selenida, elektroenapan ialah teknik yang lebih mudah, kos efektif dan boleh disediakan pada suhu rendah. Walau bagaimanapun, sebelum ini tiada kajian terperinci mengenai kesan perubahan parameter elektroenapan logam kalkogenida ini yang telah dilaksanakan. Selain itu, elektroenapan denyutan kuprum selenida tidak pernah dilaporkan. Dalam kerja ini, lapisan filem nipis kuprum selenida dielektroenapkan di atas kaca yang disaluti dengan indium timah oksida (ITO) di dalam larutan akueous berasid yang mengandungi  $\text{CuSO}_4$  dan  $\text{Na}_2\text{SeO}_3$  melalui elektroenapan potentiostatik dan teknik baru iaitu elektroenapan denyutan daripada sel tiga elektrod.

Proses elektrod dan julat keupayaan untuk penganapan kuprum selenida dikaji dengan voltametri siklik. Pencirian lapisan filem telah dijalankan dengan

menggunakan Analisis Pembelauan Sinar X (XRD), Ujian Fotoelektrokimia (PEC) dan Mikroskopi Pengimbasan Elektron (SEM). Luang tenaga optik dan jenis peralihan kuprum selenida ditentukan dengan spektrofotometer ultralembayung dan nampak (UV-vis). Sifat elektrokimia bagi enapan yang kaya dengan fasa CuSe dan Cu<sub>3</sub>Se<sub>2</sub> juga dikaji dengan teknik voltametri fasa pepejal. Sampel tertentu juga dipanas di bawah atmosfera nitrogen pada suhu yang berlainan dan dianalisis.

Pengenapan potentiostatik telah dijalankan pada keupayaan pengenapan, kepekatan Na<sub>2</sub>SeO<sub>3</sub>, masa, pH dan suhu larutan yang berlainan. XRD menunjukkan peningkatan keupayaan pengenapan dari -0.1 V ke -0.6 V, kepekatan Na<sub>2</sub>SeO<sub>3</sub> dari 0.006 M ke 0.01 M, masa pengenapan dari 1 min ke 25 min dan suhu larutan dari 0 °C ke 55 °C menggalakkan pertumbuhan fasa CuSe relatif terhadap Cu<sub>3</sub>Se<sub>2</sub>. Walau bagaimanapun, masa pengenapan yang lebih panjang, keupayaan dan suhu yang tinggi menghasilkan filem yang mempunyai kelekatan yang kurang baik. Kebanyakan parameter penyediaan nyata tidak memberi kesan kepada fotoaktiviti enapan, kecuali pH dan suhu pemanasan menunjukkan kesan yang ketara.

Pengenapan denyutan dilakukan dengan keupayaan katodik denyutan dan kitaran tugas yang berlainan. Pengenapan teknik denyutan dengan keupayaan sehingga -0.9V didapati boleh menghasilkan filem dengan kelekatan yang baik. Peningkatan keupayaan denyutan dan kitaran tugas menggalakkan pertumbuhan fasa CuSe berbanding dengan Cu<sub>3</sub>Se<sub>2</sub>. Walau bagaimanapun, kebanyakan enapan tidak sensitif terhadap cahaya.

Parameter penyediaan bagi kedua-dua kaedah telah dioptimumkan berdasarkan fotosensitiviti. Semua sampel bersifat polihablur dan menunjukkan sifat semikonduksi jenis-p daripada ujian fotoelektrokimia. Pemanasan pada suhu 400 °C menyebabkan pembentukan  $\text{Cu}_{2-x}\text{Se}$ . Pengenapan denyutan dan pemanasan yang berturutan menghasilkan enapan yang mengandungi bendasing  $\text{Cu}_2\text{O}$  di mana ruang tenaga peralihan terus diturunkan dari 1.98 eV ke 1.36 eV dan fotoarus meningkat dengan ketara.

Mikrograf SEM bagi enapan yang disediakan secara potentiostatik dan denyutan pada keupayaan yang terpilih menunjukkan morfologi permukaan dengan liputan yang baik, bebas daripada retakan dan liang seni. Kekasaran dan saiz zarah kuprum selenida meningkat dengan peningkatan keupayaan pada setiap kaedah. Filem pengenapan denyutan mempunyai morfologi permukaan yang lebih licin dan saiz zarah yang lebih kecil. Sifat elektrokimia enapan mengandungi CuSe sebagai fasa utama jelas berbeza daripada enapan yang kaya dengan  $\text{Cu}_3\text{Se}_2$  daripada kajian voltametri fasa pepejal.

## ACKNOWLEDGEMENTS

I would like to express my sincere appreciation and gratitude to my supervisor, Professor Dr. Zulkarnain Zainal and co-supervisor Associate Professor Dr. Tan Wee Tee for their invaluable advice, guidance and assistance throughout the duration of this project.

The assistance from the staffs in Chemistry Department and Institute of Bioscience was also gratefully acknowledged. I also would like to extend special thank to my friends in laboratory 2 for their assistance and guidance in operating the instruments which are essential in this study.

The financial support for this research and the fellowship scholarship are also acknowledged.

I certify that an Examination Committee has met on 12 October 2009 to conduct the final examination of Koo Chee Siong on his degree of Master of Science thesis entitled “Potentiostatic and Pulse Electrodeposition of Copper Selenide Thin Films” in accordance with Universities and University Colleges Act 1971 and the Constitution of the Universiti Putra Malaysia [P.U.(A) 106] 15 March 1998. The committee recommends that the student be awarded the Master of Science.

Members of the Thesis Examination Committee were as follows:

**Mohd Zobir Hussein, PhD**

Professor  
Faculty of Science  
Universiti Putra Malaysia  
(Chairman)

**Nor Azah Yusuf, PhD**

Associate Professor  
Faculty of Science  
Universiti Putra Malaysia  
(Internal Examiner)

**Anuar Kassim, PhD**

Professor  
Faculty of Science  
Universiti Putra Malaysia  
(Internal Examiner)

**Madzlan Aziz, PhD**

Professor  
Faculty of Science  
Universiti Teknologi Malaysia  
(External Examiner)

---

BUJANG BIN KIM HUAT, PhD  
Professor and Deputy Dean  
School of Graduates Studies  
Universiti Putra Malaysia

Date: 15 January 2010



This thesis was submitted to the Senate of Universiti Putra Malaysia and has been accepted as fulfillment of the requirement for the degree of Master of Science. The members of the Supervisory Committee were as follows:

**Zulkarnain Zainal, PhD**

Professor  
Faculty of Science  
Universiti Putra Malaysia  
(Chairman)

**Tan Wee Tee, PhD**

Associate Professor  
Faculty of Science  
Universiti Putra Malaysia  
(Member)

---

HASANAH MOHD. GHAZALI, PhD  
Professor and Dean  
School of Graduates Studies  
Universiti Putra Malaysia

Date:

## **DECLARATION**

I declare that the thesis is my original work except for quotations and citations which have been duly acknowledged. I also declare that it has not been previously, and is not concurrently, submitted for any other degree at Universiti Putra Malaysia or at any other institution.

---

**KOO CHEE SIONG**

Date:

## TABLE OF CONTENTS

	<b>Page</b>
<b>DEDICATION</b>	ii
<b>ABSTRACT</b>	iii
<b>ABSTRAK</b>	vi
<b>ACKNOWLEDGEMENTS</b>	ix
<b>APPROVAL</b>	x
<b>DECLARATION</b>	xii
<b>LIST OF TABLES</b>	xv
<b>LIST OF FIGURES</b>	xvi
<b>LIST OF ABBREVIATIONS</b>	xx
<b>CHAPTER</b>	
<b>1 INTRODUCTION</b>	
1.1 History background of photoelectrochemistry	1
1.2 Basic principles of Photoelectrochemical cell	2
1.3 Copper selenide	4
1.4 Semiconductor theory	4
1.4.1 Band structure of semiconductor	5
1.5 Electrodeposition	6
1.5.1 Potentiostatic and pulse electrodeposition	7
1.6 Electrochemical studies of solid compounds	9
1.7 Literature review	10
1.7.1 Previous works on preparation of copper selenide films	10
1.7.2 Previous works on potentiostatic deposited chalcogenide semiconductor	11
1.7.3 Previous works on pulse deposited chalcogenide semiconductor	16
1.7.4 Previous works on solid phase voltammetry of chalcogenide semiconductor	17
1.8 Problem statement	18
1.9 Objectives	19
<b>2 MATERIALS AND METHODS</b>	
2.1 Electrolytes preparation	20
2.2 Electrodes	20
2.3 Cyclic voltammetric study	21
2.4 Potentiostatic deposition of copper selenide	22
2.4.1 Deposition potential	22
2.4.2 Na <sub>2</sub> SeO <sub>3</sub> concentration	22
2.4.3 Deposition time	23
2.4.4 pH	23
2.4.5 Bath temperature	23
2.4.6 Complexing agent	23
2.4.7 Annealing temperature	24
2.5 Pulse electrodeposition of copper selenide	24

2.5.1	Cathodic pulse potential, $E_{ON}$	24
2.5.2	Duty cycles	25
2.5.3	Annealing temperature	25
2.6	Characterisations	25
2.6.1	X-ray diffraction analysis (XRD)	25
2.6.2	Photoelectrochemical test (PEC)	25
2.6.3	Morphological	26
2.6.4	Optical absorption	26
2.6.5	Solid phase voltammetry	26
<b>3</b>	<b>RESULTS AND DISCUSSION</b>	
3.1	Voltammetric studies	28
3.2	Potentiostatic electrodeposition of copper selenide	33
3.2.1	Effect of deposition potential	33
3.2.2	Effect of $Na_2SeO_3$ concentration	41
3.2.3	Effect of deposition time	46
3.2.4	Effect of pH	50
3.2.5	Effect of bath temperature	55
3.2.6	Effect of EDTA	59
3.2.7	Effect of annealing temperature	63
3.3	Pulse electrodeposition of copper selenide	67
3.3.1	Effect of pulse potential, $E_{ON}$	67
3.3.2	Effect of duty cycle	71
3.3.3	Effect of annealing temperature	74
3.4	Characterisations	77
3.4.1	Surface morphology	77
3.4.2	Optical properties	84
3.4.3	Solid phase voltammetry	88
<b>4</b>	<b>4.0 CONCLUSION</b>	<b>98</b>
	<b>4.1 RECOMMENDATION</b>	<b>100</b>
	<b>REFERENCES</b>	<b>102</b>
	<b>APPENDICES</b>	<b>114</b>
	<b>LIST OF CONFERENCES ATTENDED</b>	<b>117</b>
	<b>BIODATA OF STUDENT</b>	<b>118</b>

## LIST OF TABLES

Table		Page
1	Duty cycle, $t_{ON}$ , $t_{OFF}$ and cycles number of double pulse chronoamperometry	25
2	Voltammetric data obtained from cyclic voltammograms in Figure 8	31

## LIST OF FIGURES

Figure		Page
1	Illustration of Edmond experiment in 1839	1
2	Formation of bands in solids by assembly the isolated atoms into a lattice	5
3	Variation of energy with the crystal momentum for the direct and indirect semiconductors. The light and bold lines show the conduction band for direct and indirect semiconductors, respectively	6
4	Cathodic potential or cathodic current densities wave form of (a) Potentiostatic electrodeposition (b) Pulse electrodeposition	7
5	Variation of film thickness with time and bath temperature (bath composition: 2 mM SeO <sub>2</sub> , 1 mM HgCl <sub>2</sub> pH 3.5, deposition potential, -0.7 V vs SCE, temperature 60 °C)	14
6	PEC measurement for three In <sub>2</sub> S <sub>3</sub> samples deposited at pH 2, 2.4 and 3.5	16
7	Schematic three-electrode cell setup for cyclic voltammetry, potentiostatic and pulse electrodeposition	21
8	Figure 8: Cyclic voltammograms of ITO in: (a) 0.01 M Na <sub>2</sub> SO <sub>4</sub> (b) 0.01 M Na <sub>2</sub> SeO <sub>3</sub> (c) 0.01 M CuSO <sub>4</sub> (d) 0.01 M Na <sub>2</sub> SeO <sub>3</sub> + 0.01 M CuSO <sub>4</sub> . All electrolytes were added with 5 mL of 0.1 M H <sub>2</sub> SO <sub>4</sub> , except (a). The potential scan rate was 10 mV s <sup>-1</sup>	28
9	Chronoamperometric transients for copper selenide deposition at different potentials. (a) -0.1 V (b) -0.2 V (c) -0.3 V (d) -0.4 V (e) -0.5 V (f) -0.6 V	33
10	X-ray diffraction patterns of blank ITO and potentiostatically deposited copper selenide thin films in a sulphate solution at different deposition potentials	35
11	Linear sweep photovoltammogram of bare ITO, copper coated ITO, selenium coated ITO and copper selenide deposited potentiostatically at different deposition potentials	40
12	X-ray diffraction patterns of copper selenide thin films deposited at different Na <sub>2</sub> SeO <sub>3</sub> concentrations. The concentration of CuSO <sub>4</sub> was maintained at 0.01 M	42
13	Linear sweep photovoltammograms of copper selenide deposited at different Na <sub>2</sub> SeO <sub>3</sub> concentrations. The concentration of CuSO <sub>4</sub> was fixed at 0.01 M	44

14	Percentage of Cu and Se content of the samples deposited at varying $\text{Na}_2\text{SeO}_3$ concentrations	45
15	X-ray diffraction patterns of copper selenide deposited at different deposition time	47
16	Linear sweep photovoltammograms of copper selenide thin films deposited at different deposition time.	49
17	X-ray diffraction patterns of the films deposited at different pH	50
18	Linear sweep photovoltammograms of the samples deposited at different pH	54
19	X-ray diffraction patterns of copper selenide deposited at different bath temperatures.	55
20	Linear sweep photovoltammograms of the samples deposited at different bath temperatures. Inset shows the magnified image of photocurrent-potential curves for the samples deposited at 45 °C and 50 °C	58
21	Cyclic voltammograms of ITO in 0.01 M $\text{Na}_2\text{SeO}_3$ , 0.01 M $\text{CuSO}_4$ without EDTA (slim line) and with EDTA (bold line). The potential scan rate was $10 \text{ mV s}^{-1}$	59
22	Cyclic voltammograms of ITO in 0.01 M $\text{CuSO}_4$ + 0.01 M $\text{Na}_2\text{SeO}_3$ without EDTA (slim line) and with EDTA (bold line). The potential scan rate was $10 \text{ mVs}^{-1}$	60
23	X-ray diffraction patterns of copper selenide deposited (a) without (b) with the presence of Ethylenediamine tetraacetic acid, EDTA	61
24	Linear sweep photovoltammograms of the copper selenide deposited (a) without (b) with the presence of ethylenediamine tetraacetic acid, EDTA	62
25	X-ray diffraction patterns for deposits prepared using potentiostatic electrodeposition technique. (a) as-deposited and (b) annealed samples at different temperatures	64
26	Linear sweep photovoltammograms of as-deposited and annealed samples at different temperatures	66
27	X-ray diffraction patterns of copper selenide thin films deposited at different cathodic pulse potentials, $E_{\text{ON}}$ . The $E_{\text{OFF}}$ was fixed at 0.18 V	68

28	Linear sweep photovoltammograms of pulse-deposited copper selenide thin films at different pulse potential, $E_{ON}$ . The $E_{OFF}$ was fixed at 0.18 V	70
29	X-ray diffraction patterns of copper selenide films pulse electrodeposited at different duty cycles. $E_{ON} = -0.8$ V, deposition duration was 10 min	72
30	Linear sweep photovoltammograms of pulse-deposited copper selenide thin films at different duty cycles	73
31	X-ray diffraction patterns for deposits prepared using pulse electrodeposition technique. (a) as-deposited and (b) annealed samples at different temperatures	75
32	Linear sweep photovoltammograms of as-deposited and annealed samples at different temperatures	77
33	SEM micrographs of copper selenide thin films electrodeposited using potentiostatic [(a), (c), (e), (g)] and pulse techniques [(b), (d), (f), (h)] at -0.1 V for 10 min. Magnifications: (a) and (b) 2,000 X, (c) and (d) 5,000 X, (e) and (f) 10,000 X, (g) and (h) 15,000 X	79
34	SEM micrographs of copper selenide thin films electrodeposited using potentiostatic [(a), (c), (e), (g)] and pulse techniques [(b), (d), (f), (h)] at -0.4 V for 10 min. Magnifications: (a) and (b) 2,000 X, (c) and (d) 5,000 X, (e) and (f) 10,000 X, (g) and (h) 15,000 X.	81
35	SEM micrographs of copper selenide thin films electrodeposited using potentiostatic [(a), (c), (e), (g)] and pulse techniques [(b), (d), (f), (h)] at -0.7 V for 10 min. Magnifications: (a) and (b) 2,000 X, (c) and (d) 5,000 X, (e) and (f) 10,000 X, (g) and (h) 15,000 X.	83
36	SEM micrographs of copper selenide thin film electrodeposited using pulse technique at -0.8 V for 10 min. Magnification: (a) 2,000 X, (b) 5,000 X, (c) 10,000 X and (d) 15,000 X	84
37	Absorption spectrum of $Cu_{2-x}Se$ film coated onto ITO	85
38	Plot of $(Ah\nu)^2$ versus $h\nu$ for $Cu_{2-x}Se$ film coated onto ITO	86
39	Absorption spectrum of mixed phase of $Cu_{2-x}Se$ and $Cu_2O$ film coated onto ITO	87
40	Plot of $(Ah\nu)^2$ versus $h\nu$ for mixed phase of $Cu_{2-x}Se$ and $Cu_2O$ film coated onto ITO	87
41	Cyclic voltammogram of $CuSO_4$ powder mechanically attached to a glassy carbon electrode and immersed in 0.1 M $KNO_3$ . Potential scan rate was $20 \text{ mV s}^{-1}$ . The number of scan cycle was 10	88

42	Cyclic voltammograms of copper selenide mechanically attached to a 3 mm diameter glassy carbon electrode and immersed in 0.1 M KNO <sub>3</sub> . Potential scan rate was 20 mV s <sup>-1</sup> . The number of scan cycle was 10. (a) CuSe rich phase (b) Cu <sub>3</sub> Se <sub>2</sub> rich phase	89
43	Cyclic voltammograms of CuSe rich phase sample mechanically attached to a 3 mm diameter glassy carbon electrode and immersed in 0.1 M KNO <sub>3</sub> . Potential scan rate was 20 mV s <sup>-1</sup> . The number of scan cycle was 10	92
44	Cyclic voltammograms of Cu <sub>3</sub> Se <sub>2</sub> rich phase sample mechanically attached to a 3 mm diameter glassy carbon electrode and immersed in 0.1 M KNO <sub>3</sub> . Potential scan rate was 20 mV s <sup>-1</sup> . The number of scan cycle was 10	93
45	Anodic differential pulse voltammograms of (a) CuSe (b) Cu <sub>3</sub> Se <sub>2</sub> rich phase in 0.1 M KNO <sub>3</sub> . Potential scan rate was 10.5 mV s <sup>-1</sup> , step potential = 0.00105 V. Interval time = 0.1 s. Modulation time = 0.05 s	95
46	Cathodic differential pulse voltammograms of (a) CuSe (b) Cu <sub>3</sub> Se <sub>2</sub> rich phase in 0.1 M KNO <sub>3</sub> . Potential scan rate was 10.5 mV s <sup>-1</sup> , step potential = 0.00105 V. Interval time = 0.1 s. Modulation time = 0.05 s	97
47	SEM images of opper selenide deposited at -0.1 V using (a) potetiostatic and (b) pulse techniques	114
48	SEM images of copper selenide deposited at -0.4 V using (a) potetiostatic and (b) pulse techniques	115
49	SEM images of copper selenide deposited at (a) -0.7 V and (b) -0.8 V using pulse tecnnique	116

## LIST OF ABBREVIATIONS

Ag/AgCl	Silver/ Silver chloride
DPV	Differential Pulse Voltammogrametry
EDTA	Ethylenediamine Tetraacetic Acid
$E_g$	Band Gap Energy
$E_{OFF}$	Zero Current Potential
$E_{ON}$	Cathodic Pulse Potential
Eq.	Equation
FTO	Fluoride Tin Oxide
ICP-AES	Inductively Coupled Plasma Atomic Emission Spectrometer
ITO	Indium Tin Oxide
$i-V$	Current-Potential
JCPDS	Joint Committee of Powder Diffraction Standard
$J_{oc}$	Short Circuit Current Densities
MOCVD	Metal Organic Chemical Vapor Veposition
PEC	Photoelectrochemical Test
SEM	Scanning Electron Microscopy
$t_{ON}$	Duration of Cathodic Pulse Potential
$t_{OFF}$	Duration of Zero Current Potential
$V_{oc}$	Open Circuit Potential
XRD	X-ray Diffraction



# CHAPTER 1

## INTRODUCTION

### 1.1 History background of photoelectrochemistry

The growing interest in photoelectrochemistry has been stimulated by concern over the depletion of global fossil fuel. Solar energy conversion to electricity and chemical fuels can be achieved via photoelectrochemical cell (Wrighton, 1979). Photoelectrochemistry is nothing new. Nearly two centuries ago, a French physicist, Edmond Becquerel discovered the illuminated silver halide electrode immersed in acid, neutral and basic electrolyte generated small electric current through external circuit (Honda, 2004; Gerischer, 1975). The counter electrodes used were Pt, Au, Ag and Brass. Edmond Becquerel's experiment is illustrated in Figure 1.

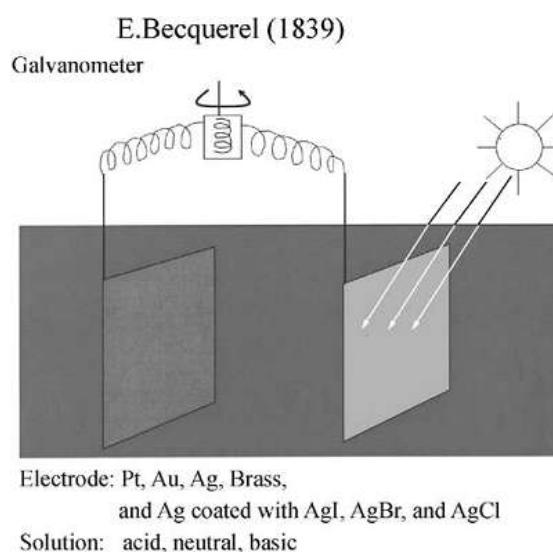


Figure 1: Illustration of Edmond experiment in 1839. *Reproduced from Honda (2004).*

This was the first observation of semiconductor photoelectrochemical energy conversion. However, research in this field received considerable attention only after 1970s.

Fujishima and Honda (1972) decomposed water into hydrogen and oxygen using *n*-type TiO<sub>2</sub>. Their finding prompted scientists around the world to involve in the field. Although TiO<sub>2</sub> is stable against photocorrosion, but its band gap is 3.2 eV means only UV light is absorbed.

Hodes *et al.* (1976) reported the use of electrolytic deposited CdSe as liquid junction solar cell. At the same year, Miller and Heller from the Bell Laboratories also independently studied the CdS and Bi<sub>2</sub>S<sub>3</sub> photoelectrochemical solar cell. Liquid junction solar cell provides easier ways to form rectifying junctions comparatively to costly and sophisticated solid state processing techniques (Bard, 1980). The junction is produced by immersing the semiconductor in solution. Moreover, semiconductors with *n*-type or *p*-type character is suitable used for photoelectrochemical electrode, provided their band gap energy matches the solar spectrum (Finklea, 1983; Bard, 1980). This exciting idea continues to drive research in this area.

## 1.2 Basic principles of photoelectrochemical cell

The basic principles of such liquid junction semiconductor device involve:

- (a) Photon captures by semiconductor and cause the transition of electron from valance band to conduction band. The wavelength of light should equal to or greater than the band gap energy  $E_g$  to cause such a transition. The wavelength  $\lambda$  can be calculated according to Eq. (1) (Finklea, 1983).

$$\lambda(\text{nm}) \geq \frac{1240}{E_g} \quad \text{Eq. (1)}$$

(b) The result of photon absorption is an electron-hole pair ( $e^-h^+$ ) formation. If  $e^-h^+$  pair can be separated so that the  $e^-$  flows to a suitable acceptor species, A



or an electron from a suitable donor, D, fills  $h^+$  in the solution.



The light energy has been stored, at least for a short time, as redox chemical energy.

(c) If  $e^-$  is pumped through a wire, it has been converted to an electrical current. However,  $e^-h^+$  pairs frequently recombine very quickly with the captured light degraded to heat or sometimes with the emission of a photon, as in phosphorescence (Bard, 1980).

Therefore, to utilize the light in electricity generation other than heat, the  $e^-h^+$  pairs separation must achieve to minimize the recombination. This separation can be promoted by applying the bias potential across the semiconductor electrode (Bard, 1980). Some excellent reviews on the theory of semiconductor photoelectrochemistry are available and therefore will not be discussed in detail here (Honda, 2004; Bard, 1980; Wrighton, 1979; Gerischer, 1957). In this area of research, new methods and new materials are being explored, to prepare the semiconductor electrode in a simple and cost effective way. Solar energy can be effectively harvested using an electrode in the form of thin film. Furthermore, thin film electrode only requires small amount of solid to be deposited and hence the production cost is reduced.

### 1.3 Copper selenide

Copper selenide is an interesting p-type semiconductor which has wide variety of stoichiometric composition due to existing two oxidation states of copper ion. They exist in numerous phases and structural forms as stoichiometric CuSe, CuSe<sub>2</sub>, Cu<sub>2</sub>Se, Cu<sub>3</sub>Se<sub>2</sub> and as well as non-stoichiometric Cu<sub>2-x</sub>Se (Heyding and Murray, 1976; Murray and Heyding, 1975; Heyding 1966).

Various promising applications of copper selenide in photovoltaic devices (Cao *et al.*, 2007; Ambade *et al.*, 2006; Chen *et al.*, 1985; Okimura and Matsume, 1980; Tell and Wiegand, 1977), superionic conductor (Kourzhuer, 1998; Kashida and Akai; 1988), rechargeable lithium battery (Xue *et al.*, 2006), ion selective microelectrode (Papeschi *et al.*, 2000; Papeschi *et al.*, 1992) and Shottky diodes (Brien and Santhanam, 1989) attract the interest of researchers towards this material. The compound is also an interesting precursor to synthesis CuInSe<sub>2</sub> (Oliveira *et al.*, 2002; Brien and Santhanam, 1992; Baumerzoug and Dao, 1990). Since indium has poor surface affinity to indium tin oxide coated glass (ITO) surface (Baumerzoug and Dao, 1990; Battacharya and Rajeshwar, 1986). Hence, two steps electrodeposition is required to obtain nearly stoichiometric CuInSe<sub>2</sub>/ITO film (Baumerzoug and Dao, 1990).

### 1.4 Semiconductor theory

Photoelectrochemistry is based principally on the semiconductor electrode. To understand the subject, some simple concepts of solid state physics must be discussed. The band model is usually used to describe the electronic properties of solids. The isolated atoms are characterized by filled and vacant orbitals. When these